JOURNAL OF CHEMICAL & ENGINEERING DATA

ARTICLE

pubs.acs.org/jced

Speed of Sound in Liquid Water from (253.15 to 348.15) K and Pressures from (0.1 to 700) MPa

Eduardo Hidalgo Baltasar,[†,§] Mercedes Taravillo,[†,§] Valentín G. Baonza,[†,§] Pedro D. Sanz,[‡,§] and Bérengère Guignon*[,‡]

[†]MALTA-Consolider Team, Departamento de Química Física I, Facultad de Ciencias Químicas, Universidad Complutense de Madrid, 28040 Madrid, Spain

[‡]MALTA-Consolider Team, Departamento de Procesos, Instituto de Ciencia y Tecnología de Alimentos y Nutrición, ICTAN - CSIC, C/José Antonio Nováis 10, 28040 Madrid, Spain

ABSTRACT: Water thermodynamic properties are available as standards through the IAPWS-95 formulation of the equation of state. Among these properties, speed of sound is very useful for calibrating devices and for obtaining derived properties. However, the values of speed of sound calculated in the range (200 to 700) MPa are more uncertain than desirable, due to a lack of accurate experimental data above 200 MPa. The aim of this work is to provide a complete set of accurate speed of sound results in water covering the pressure range mentioned above. Speed of sound was determined by the multiple reflections method between (0.1 and 700) MPa at temperatures from (253.15 to 348.15) K. Estimated uncertainties at a confidence level of 95 % range between (0.22 and 0.32) % over the whole pressure range. These new results may help to improve the reference database for future parametrizations of the equation of state for water.

INTRODUCTION

Liquid water has been subjected to many types of investigations for a long time due to its role in many biological, physical, and chemical phenomena and because of its importance in industrial processes. As a reference fluid, it is often used to calibrate apparatus or to compare data; the numerical simulation of any industrial process involving water also requires a precise knowledge of all its properties as a function of both pressure and temperature.[1] Thus, the scientific community continuously needs to access to water properties in a practical, versatile, and standardized fashion. Many efforts were made in this way, and different equations of state of liquid water have been proposed over time. As a result, in 1995 the International Association for Properties of Water and Steam (IAPWS) adopted the equation of state for water still in use to date. The so-called IAPWS-95 formulation[2] is based on the Helmholtz free energy, and it is periodically revised.

Speed of sound is a key quantity in equation of state formulations because it is used to estimate other thermodynamic properties (e.g., specific heat) or to study kinetic phenomena.[3] Many accurate data of speed of sound in water at pressures below 200 MPa are available to date, but results at higher pressures are scarcer. Techniques employed for ultrasound measurements were mainly the pulse-echo method below 200 MPa[4−6] and Brillouin scattering method in diamond anvil cell between (1 and 25) GPa.[7−9] However, at intermediate pressures, only a few results[10−12] were available at that time, and only those reported by Holton et al.[10] at 323 K were selected to fit the coefficients of the IAPWS-95 equation of state. As a consequence, the uncertainty in the calculated speed of sound in the (200 to 1000) MPa range is relatively large. Furthermore, the uncertainty is still unknown above 323.15 K in this pressure range, so a new set of speed of sound data in the low-temperature and intermediate pressure regime was demanded. Recently Vance et al.[13] published new speed of sound data within the range of interest by the impulsive stimulated scattering technique using a sapphire-window cell. They claimed uncertainties about (0.2 to 0.3) % and noted deviations from the IAPWS-95 at (323.15 and 373.15) K above (200 to 300) MPa, while their data agreed with the IAPWS-95 at the lowest temperatures. Here we employed the multiple reflections method to provide with a complete set of speed-of-sound measurements in liquid water covering pressures between (200 and 700) MPa and temperatures between (253.15 and 348.15) K. In contrast with the results of Vance and Brown[13] we find systematic deviations from the IAPWS-95 formulation at temperatures below room temperature.

MATERIALS AND METHODS

Setup for Ultrasonic Measurements. Ultrasonic measurements were performed by the multiple reflections method. The ultrasound cell was designed to fit with the characteristics of our laboratory high-pressure equipment. A detailed description of the high-pressure setup has been published elsewhere.[14] The different elements of the cell are shown in Figure 1. The transmitter and receiver piezoelectric ceramics (10 mm diameter, 1 mm thick, main resonance frequency 2 MHz, Ferroperm, Denmark) were placed parallel to each other in the vertical position. Each piezoelectric ceramic was sandwiched between two polytetrafluoroethylene masks and fixed with a rubber O-ring. These elements were tightly held in front of each other with two stainless steel screws

Special Issue: Kenneth N. Marsh Festschrift

Received: July 26, 2011
Accepted: October 30, 2011
Published: November 14, 2011

ACS Publications © 2011 American Chemical Society

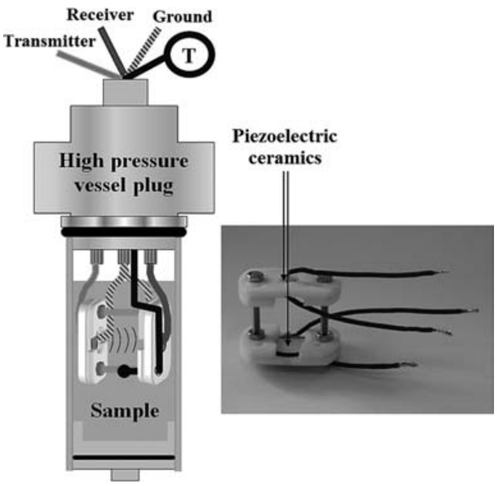

Figure 1. Ultrasound measurement cell.

and nuts. Four cables were welded to the piezoelectric ceramic surface: one for pulse emission, one for electric signal reception, and the two others for ground. These cables were connected to a high pressure vessel plug specifically designed for electric measurements (UNIPRESS, Institute of High Pressure Physics, Warsaw, Poland). The plug was also provided with a T-type thermocouple and a cylindrical stainless steel sample holder (24 mm diameter, 17 cm^3 capacity). The thermocouple tip was located below the piezoelectric ceramics avoiding the ultrasounds measurement zone. The sample holder includes a movable piston. The setup was completed by a pulse generator (model 5072PR, Panametrics, Tech Instruments Inc., Waltham, MA, USA) for electric pulse emission and an oscilloscope (TDS 5032B digital phosphor oscilloscope 350 Hz, 5 GSample/s, Tektronix, Beaverton, OR, USA) for electric signal reception. Coaxial cables were used for electric connections between the ultrasound cell and these apparatus to avoid electric noise. The temperature was controlled using a thermostatic bath (Haake K, Karlsruhe, Germany) with a stability better than 0.05 K. The pressure was measured with a strain gauge transducer (EBM 6045 V-0-10 GmbH, KGT Kramer, Dortmund, Germany). The temperature and pressure were recorded every 2 s by using a data acquisition system (DC100 Data Collector Yokogawa, Tokyo, Japan). The estimated uncertainties of these measurements are fully derived in the Results and Discussion section.

Experimental Procedure. The sample holder was filled with about 17 mL of deionized water type I (electrolytic conductivity $\sim$0.05 $\mu S \cdot cm^{-1}$, Milli-Q system, Millipore, Billerica, MA, USA) and degassed using an ultrasonic bath (model 3000515, J.P. Selecta S.A., Barcelona, Spain). The ultrasound cell was introduced in the sample holder, and a layer of silicone oil about 10 mm thick was added to isolate electric connections from the water sample. Silicone oil was also used as the pressure transmitting fluid. This assembly was placed on the high pressure vessel, and the plug was screwed home to fully close the vessel which was subsequently immersed in a water bath. Temperature stability was typically achieved in less than two hours. Then pressure was slowly increased up to 700 MPa in (5, 10, 25, or 50) MPa steps, and the temperature was equilibrated to release the heat generated during each compression step. The oscilloscope signal was then recorded after averaging 5000 waveforms at a 800 ps resolution. Pressure and temperature values were averaged from measurements taken every 2 s during 44 s after temperature equilibration. The repeatability of these measurements was always less than $\pm$ 0.3 MPa and $\pm$ 0.19 K, respectively. This procedure was repeated up to three times at each temperature.

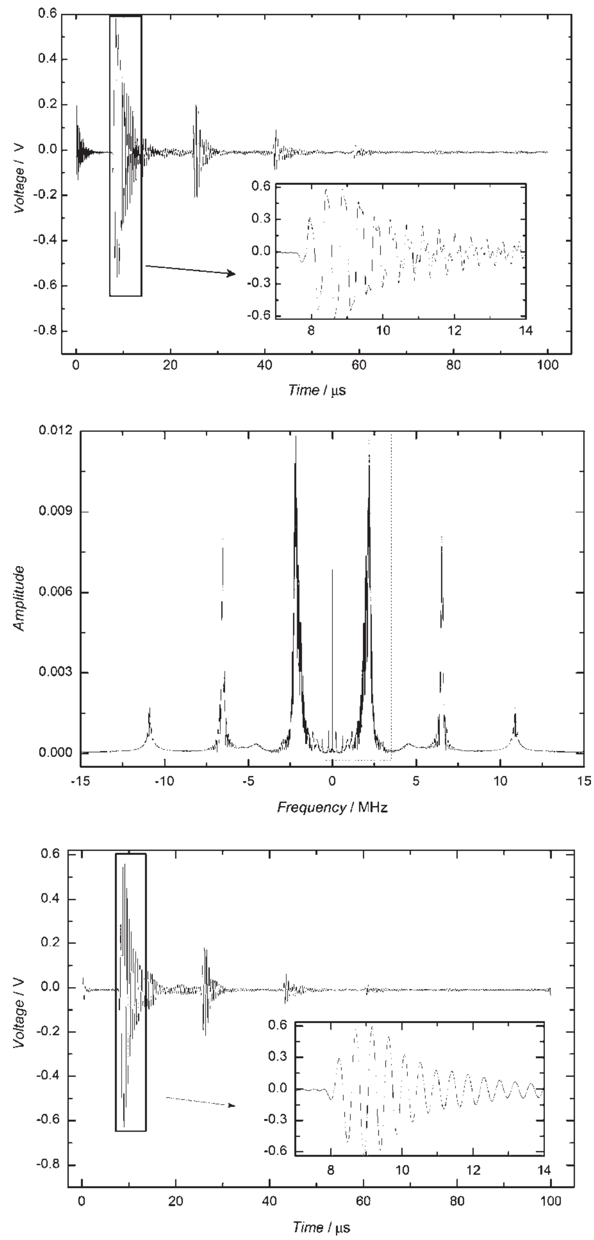

Figure 2. Steps of signal treatment. (a) Acquired electric signal. (b) Fast Fourier transformed signal. (c) Treated signal and identification of echoes positions.

Signal Treatment. The signal was analyzed using the OriginPro 8.0 package (OriginLab Corporation, Northampton, MA, USA). Figure 2a shows an example of the recorded signal. About five echoes of decreasing amplitude are typically observed in the whole waveform. The time of fight τ (interval between echoes) corresponds to one round trip (i.e., twice the distance between piezoelectric ceramics). A fast Fourier transform (FFT) filter was applied to eliminate unwanted frequencies on the recorded signal (see Figure 2b) by limiting the data corresponding to the main resonance frequency of the piezoelectric ceramics (2 MHz) and finally calculating the inverse Fourier transform of the selected

dx.doi.org/10.1021/je200668a |J. Chem. Eng. Data 2011, 56, 4800–4807

data. A band-pass filter between (0 and 3) MHz allowed for an unambiguous determination of the maxima and minima positions in the waveform (see Figure 2c).

Calibrations. The thermocouple was calibrated against two Pt100 reference thermometers (TESTO, model 735-2 and model 950, Germany) with an uncertainty better than 0.09 K, depending on the temperature considered. The pressure transducer was calibrated by the provider (KGT Kramer, Dortmund, Germany) with a relative uncertainty of 0.5 %.

The distance between the piezoelectric ceramics was calibrated at 50 MPa for $T \geq 273.15$ K and at the first pressure of measurement for $T < 273.15$ K (i.e. 75 MPa at 268.15 K, 125 MPa at 263.15 K, 175 MPa at 258.15 K, and 200 MPa at 253.15 K). We preferred to calibrate the distance between the piezoelectric ceramics under pressure to avoid inaccuracies due to the presence of air bubbles at room pressure. The reference pressures selected at each temperature were high enough to avoid such an effect but as close as possible to the crystallization pressure. The high accuracy of IAPWS-95 formulation at these relatively low pressures guarantees the goodness of our calibration.

The time-of-flight at the calibration conditions, τ_{cal}, was multiplied by the speed of sound, w_{cal}, calculated from the IAPWS-95 at the same temperature and pressure conditions.[2] Thus:

$$d_{cal} = w_{cal}(p_{cal}, T_{cal}) \cdot \frac{\tau_{cal}}{2} \quad (1)$$

where d_{cal} represents the distance between piezoelectric pieces at the pressure and temperature of the calibration.

The deformation of the cell screws was considered to refine the distance at any other pressure p than that of calibration, d_p, using the relationship:

$$d_p = d_{cal} \frac{1 - \frac{p(1-2\mu)}{E}}{1 - \frac{p_{cal}(1-2\mu)}{E}} \quad (2)$$

where μ is the Poisson coefficient and E is Young's modulus which, for stainless steel, take the values 0.3 and 193 GPa, respectively.

Speed of Sound Calculation. The speed of sound at a given pressure can be obtained from the measured time-of-flight τ_p and the distance between piezoelectric ceramics d_p using the equation:

$$w(p) = \frac{2d_p}{\tau_p} \quad (3)$$

Or more explicitly in terms of measured quantities:

$$w(p) = \frac{\tau_{cal}}{\tau_p} \frac{1 - p\left(\frac{1-2\mu}{E}\right)}{1 - p_{cal}\left(\frac{1-2\mu}{E}\right)} w_{cal} \quad (4)$$

RESULTS AND DISCUSSION

Estimated Uncertainties. The combined standard uncertainties in both temperature and pressure were calculated, respectively, as follows:

$$u_c(T) = \left[u^2(T_u) + u^2(T_{cal}) + u^2(T_{rep})\right]^{1/2} \quad (5)$$

$$u_c(p) = \left[u^2(p_u) + u^2(p_{cal}) + u^2(p_{rep})\right]^{1/2} \quad (6)$$

In each case, the first term is the uncertainty given in sensor specifications, the second term is the uncertainty of calibration, and the third term is the repeatability of our measurements. The overall result gives $u_c(T) = 0.14$ K at most for the temperature combined standard uncertainty and $u_c(p) = 0.005p$ MPa for pressure. Assuming that the possible estimated values of T and p are approximately normally distributed within the respective intervals defined by the above combined standard uncertainties ($u_c(T)$ and $u_c(p)$), the unknown values of T and p are believed to lie in these respective intervals with a confidence level of about 68 %.

The combined standard uncertainty in the speed of sound was evaluated from the following relationship:

$$u_c(w) = \left[u^2(w) + u^2(w_{uT}) + u^2(w_{up})\right]^{1/2} \quad (7)$$

where $u(w)$ is the combined standard uncertainty in speed of sound measurement and $u(w_{uT})$ and $u(w_{up})$ are the uncertainties in w due to the uncertainty in the temperature and pressure measurements, respectively.

The uncertainty $u(w)$ was calculated by applying the law of propagation of uncertainty to eq 4:

$$u(w) = \left[\left(\frac{\partial w}{\partial \tau_{cal}}\right)^2 u^2(\tau_{cal}) + \left(\frac{\partial w}{\partial \tau_p}\right)^2 u^2(\tau_p) + \left(\frac{\partial w}{\partial w_{cal}}\right)^2 u^2(w_{cal}) + \left(\frac{\partial w}{\partial p_{cal}}\right)^2 u^2(p_{cal}) + \left(\frac{\partial w}{\partial p}\right)^2 u^2(p)\right]^{1/2} \quad (8)$$

This gives:

$$u(w) = \frac{\tau_{cal}}{\tau_p} \frac{1 - p\left(\frac{1-2\mu}{E}\right)}{1 - p_{cal}\left(\frac{1-2\mu}{E}\right)} w_{cal} \cdot \left[\frac{u^2(\tau_{cal})}{\tau_{cal}^2} + \frac{u^2(\tau_p)}{\tau_p^2} + \frac{u^2(w_{cal})}{w_{cal}^2} + \left(\frac{1-2\mu}{E}\right)^2 \left(\frac{u^2(p_{cal})}{\left(1 - p_{cal}\left(\frac{1-2\mu}{E}\right)\right)^2} + \frac{u^2(p)}{\left(1 - p\left(\frac{1-2\mu}{E}\right)\right)^2}\right)\right]^{1/2} \quad (9)$$

The evaluation of the uncertainties $u(\tau_{cal})$, $u(\tau_p)$, and $u(w_{cal})$ is detailed below.

$u(\tau_{cal})$ and $u(\tau_p)$ represent the combined standard uncertainty in the time-of-flight τ determined at the pressure of distance calibration and at the pressure of measurement, respectively. These uncertainties take into account the uncertainty related to the oscilloscope horizontal setting chosen for resolution $u(\tau_u)$ and the uncertainty in repeatability from three pairs of echoes $u(\tau_{rep})$, that is:

$$u(\tau) = \left[u^2(\tau_u) + u^2(\tau_{rep})\right]^{1/2} \quad (10)$$

dx.doi.org/10.1021/je200668a | J. Chem. Eng. Data 2011, 56, 4800–4807

Table 1. Experimental Speed of Sound in Water above 273.15 K

p (MPa)	T (K)	w ($m \cdot s^{-1}$)	$u_c(w)$ ($m \cdot s^{-1}$)	p (MPa)	T (K)	w ($m \cdot s^{-1}$)	$u_c(w)$ ($m \cdot s^{-1}$)
			T = 278.15 K				
0.1	278.24	1425.6	1.8	400.0	278.09	2087.5	3.1
50.6	278.21	1510.2	1.8	450.9	278.08	2156.9	3.3
109.2	278.19	1614.9	2.1	500.3	278.05	2220.9	3.4
159.9	278.19	1705.3	2.3	550.6	278.13	2284.7	3.5
200.8	278.12	1777.1	2.5	599.3	278.17	2344.6	3.7
250.6	278.13	1859.7	2.7	651.9	278.17	2402.7	3.8
300.5	278.16	1940.0	2.8	701.3	278.17	2451.0	3.9
349.3	278.07	2013.6	3.0	0.1	278.05	1425.1	1.8
400.0	278.08	2086.4	3.1	49.2	278.09	1507.3	1.8
449.7	278.09	2155.5	3.3	99.9	278.16	1599.9	2.1
500.5	278.09	2221.3	3.4	150.1	278.14	1689.2	2.3
561.5	278.11	2297.2	3.6	200.1	278.13	1776.7	2.5
602.1	278.08	2346.8	3.7	250.1	278.13	1859.7	2.7
640.2	278.11	2390.8	3.8	299.9	278.12	1939.6	2.8
700.2	278.09	2439.8	3.9	349.8	278.17	2017.6	3.0
0.1	278.15	1424.8	1.8	400.5	278.10	2089.8	3.2
48.3	278.13	1506.0	1.8	450.8	278.12	2157.8	3.3
99.6	278.15	1597.6	2.1	500.4	278.10	2223.3	3.4
150.1	278.13	1688.3	2.3	550.8	278.09	2286.8	3.6
200.3	278.08	1775.7	2.5	600.7	278.12	2347.6	3.7
250.2	278.12	1858.4	2.7	650.0	278.12	2402.2	3.8
299.9	278.10	1938.9	2.8	700.6	278.19	2446.5	3.9
349.6	278.08	2014.7	3.0				
			T = 288.15 K				
0.1	288.11	1461.4	1.8	250.0	288.12	1878.5	2.7
50.8	288.08	1549.6	1.8	299.8	288.11	1952.9	2.9
110.9	288.09	1650.2	2.2	349.6	288.09	2026.1	3.0
160.1	288.09	1733.4	2.4	401.3	288.17	2098.0	3.2
200.8	288.11	1799.7	2.5	499.7	288.10	2225.7	3.4
250.9	288.13	1878.5	2.7	599.5	288.09	2345.8	3.7
300.7	288.07	1953.9	2.9	699.8	288.08	2453.6	3.9
350.8	288.08	2026.4	3.0	0.1	288.13	1462.4	1.8
400.3	288.08	2094.6	3.2	50.9	288.15	1550.1	1.8
450.3	288.00	2162.1	3.3	99.8	288.16	1631.8	2.1
499.8	288.15	2225.2	3.4	150.3	288.14	1718.5	2.3
561.3	288.17	2300.1	3.6	200.3	288.12	1800.1	2.5
599.9	288.11	2344.8	3.7	250.5	288.08	1878.9	2.7
640.7	288.17	2391.2	3.8	300.4	288.13	1955.1	2.9
700.8	288.11	2455.2	3.9	349.2	288.15	2025.9	3.0
0.1	288.08	1463.4	1.7	399.8	288.12	2094.8	3.2
50.9	288.09	1549.8	1.8	499.5	288.10	2226.5	3.4
99.7	288.17	1633.2	2.1	600.9	288.07	2346.8	3.7
149.8	288.08	1717.5	2.3	701.0	288.13	2453.9	3.9
200.2	288.16	1800.9	2.5				
			T = 298.15 K				
0.1	298.35	1492.8	1.8	400.5	298.15	2103.8	3.2
50.2	298.34	1580.9	1.9	450.3	298.18	2167.6	3.3
100.4	298.36	1664.2	2.2	500.0	298.15	2229.8	3.4
150.8	298.30	1745.0	2.4	551.3	298.11	2287.0	3.6

Table 1. Continued

p (MPa)	T (K)	w ($m \cdot s^{-1}$)	$u_c(w)$ ($m \cdot s^{-1}$)	p (MPa)	T (K)	w ($m \cdot s^{-1}$)	$u_c(w)$ ($m \cdot s^{-1}$)
199.8	298.34	1820.7	2.5	599.2	298.10	2344.5	3.7
249.2	298.29	1894.6	2.7	659.8	298.09	2412.6	3.8
299.0	298.30	1965.7	2.9	699.9	298.07	2450.3	3.9
350.9	298.28	2038.4	3.0	0.1	297.90	1493.8	1.8
400.4	298.24	2102.3	3.2	50.6	297.88	1580.3	1.9
449.9	298.42	2165.5	3.3	99.5	297.99	1660.6	2.2
499.7	298.43	2225.8	3.4	151.0	297.88	1743.2	2.4
549.2	298.43	2287.7	3.6	200.2	297.84	1819.5	2.5
601.8	298.45	2347.7	3.7	250.3	297.79	1895.5	2.7
651.7	298.41	2400.7	3.8	300.3	297.83	1967.2	2.9
699.0	298.38	2448.0	3.9	349.2	298.05	2035.4	3.0
0.1	298.37	1492.2	1.8	400.3	297.89	2101.3	3.2
50.1	298.20	1580.4	1.9	450.5	297.90	2165.2	3.3
100.4	298.31	1662.8	2.2	499.5	297.80	2225.4	3.4
150.7	298.27	1743.9	2.4	549.7	297.79	2286.1	3.6
200.8	298.16	1821.6	2.5	601.7	297.82	2346.1	3.7
250.7	298.31	1897.4	2.7	653.2	297.78	2402.2	3.8
300.5	298.16	1968.4	2.9	702.2	297.74	2448.7	3.9
350.6	298.12	2038.7	3.0				
			T = 308.15 K				
0.1	308.15	1514.3	1.9	400.0	308.09	2112.1	3.2
50.6	308.22	1605.5	1.9	449.3	308.07	2173.3	3.3
111.0	308.16	1706.1	2.2	499.4	308.15	2232.5	3.4
160.1	308.11	1781.2	2.4	549.7	308.17	2292.4	3.6
200.7	308.12	1840.1	2.6	601.7	308.10	2349.8	3.7
250.8	308.15	1913.1	2.7	650.7	308.11	2402.3	3.8
300.5	308.08	1983.1	2.9	703.6	308.09	2441.6	3.9
350.9	308.10	2048.9	3.1	0.1	308.15	1514.1	1.9
400.7	308.12	2110.8	3.2	51.0	308.13	1606.0	1.9
449.9	308.14	2171.7	3.3	99.8	308.17	1690.0	2.2
499.5	308.09	2230.5	3.4	150.3	308.14	1766.1	2.4
559.7	308.09	2301.4	3.6	200.3	308.17	1839.8	2.6
599.6	308.13	2344.5	3.7	250.5	308.10	1913.4	2.7
639.8	308.16	2388.9	3.8	299.9	308.10	1983.2	2.9
701.6	308.14	2447.4	3.9	349.4	308.09	2048.7	3.1
0.1	308.11	1515.3	1.9	400.4	308.06	2112.6	3.2
50.3	308.17	1604.9	1.9	450.9	308.15	2174.9	3.3
99.7	308.14	1690.4	2.2	499.7	308.21	2232.3	3.4
149.9	308.12	1766.1	2.4	549.6	308.19	2291.0	3.6
200.4	308.12	1840.6	2.6	599.6	308.22	2346.6	3.7
250.5	308.19	1913.9	2.7	650.8	308.09	2402.2	3.8
299.9	308.12	1984.1	2.9	698.5	308.10	2446.7	3.9
349.8	308.13	2049.7	3.1				
			T = 318.15 K				
0.1	317.92	1530.3	1.9	399.6	318.13	2121.7	3.2
49.1	318.26	1621.2	1.9	449.8	318.10	2181.8	3.3
99.7	318.21	1706.9	2.2	499.9	318.19	2239.9	3.5
150.4	318.22	1788.9	2.4	559.3	318.16	2305.4	3.6
200.2	318.19	1861.8	2.6	599.6	318.12	2346.3	3.7
250.0	318.15	1930.6	2.8	641.8	318.12	2388.1	3.8
300.1	318.10	1998.9	2.9	701.8	318.14	2454.2	3.9
349.6	318.09	2062.1	3.1	0.1	318.21	1530.2	1.9

Table 1. Continued

p	T	w	$u_c(w)$	p	T	w	$u_c(w)$
MPa	K	$m \cdot s^{-1}$	$m \cdot s^{-1}$	MPa	K	$m \cdot s^{-1}$	$m \cdot s^{-1}$
399.7	318.06	2122.5	3.2	50.0	318.17	1622.5	1.9
449.7	318.14	2182.1	3.3	99.5	318.07	1705.7	2.2
499.8	318.17	2240.9	3.5	150.1	318.11	1787.1	2.4
549.2	318.16	2297.1	3.6	200.4	318.10	1860.8	2.6
599.1	318.12	2350.3	3.7	250.4	318.13	1930.2	2.8
651.0	318.15	2405.8	3.8	299.4	318.10	1995.8	2.9
701.7	318.19	2454.7	3.9	349.6	318.10	2061.0	3.1
0.1	318.16	1530.9	1.9	401.3	318.16	2123.6	3.2
50.4	318.12	1623.1	1.9	450.6	318.18	2183.6	3.3
111.2	318.14	1725.7	2.3	499.1	318.17	2239.1	3.5
160.1	318.11	1802.4	2.5	549.4	318.17	2295.5	3.6
200.6	318.02	1860.6	2.6	602.1	318.21	2348.1	3.7
250.6	318.11	1930.2	2.8	651.2	318.19	2401.2	3.8
299.9	318.12	1996.4	2.9	702.4	318.18	2453.8	3.9
350.8	318.02	2062.0	3.1				
			$T = 328.15$ K				
0.1	328.27	1542.1	1.9	399.7	328.16	2133.0	3.2
50.9	328.14	1636.9	1.9	449.8	328.21	2189.2	3.3
100.1	328.12	1720.7	2.2	499.4	328.16	2246.5	3.5
150.0	328.10	1799.2	2.4	560.5	327.96	2312.8	3.6
200.2	328.13	1875.4	2.6	601.2	328.16	2355.9	3.7
250.7	328.19	1947.4	2.8	641.4	327.92	2396.1	3.8
300.0	328.15	2015.6	2.9	701.7	327.97	2451.4	3.9
351.7	328.16	2077.1	3.1	0.1	328.76	1543.9	1.9
400.1	328.22	2137.3	3.2	50.9	328.73	1637.5	1.9
450.9	328.14	2192.0	3.3	99.8	328.49	1720.6	2.3
499.6	328.08	2246.7	3.5	150.1	328.83	1799.9	2.4
550.7	328.07	2301.2	3.6	200.1	328.72	1874.3	2.6
601.9	328.16	2353.3	3.7	250.1	328.90	1944.4	2.8
652.7	328.21	2406.9	3.8	300.0	328.69	2012.1	3.0
700.1	328.16	2453.2	3.9	350.9	328.77	2076.6	3.1
0.1	328.19	1541.1	1.9	400.5	328.72	2138.4	3.2
50.6	328.17	1636.4	1.9	449.2	328.74	2194.3	3.4
109.2	328.08	1735.6	2.3	499.4	328.92	2250.4	3.5
159.9	328.16	1816.0	2.5	551.0	328.72	2304.7	3.6
200.9	328.17	1876.4	2.6	601.3	328.76	2354.9	3.7
250.7	328.18	1946.5	2.8	650.7	328.66	2404.5	3.8
300.8	328.14	2013.9	2.9	700.4	328.77	2453.8	4.0
350.7	328.08	2075.4	3.1				
			$T = 338.15$ K				
0.1	338.02	1547.4	1.7	399.1	337.69	2142.9	2.8
50.1	337.87	1643.6	1.9	451.0	338.12	2203.4	2.9
100.5	337.95	1731.6	2.0	501.1	337.80	2260.0	3.0
150.0	337.66	1810.9	2.2	549.6	338.22	2309.8	3.1
200.5	337.75	1886.0	2.3	601.1	338.04	2360.1	3.2
250.3	338.15	1956.7	2.5	650.6	338.07	2410.2	3.3
300.7	337.85	2024.0	2.6	700.8	338.22	2455.7	3.4
350.5	337.69	2086.1	2.7				
			$T = 348.15$ K				
0.1	349.19	1549.0	1.7	400.7	349.28	2153.0	2.9
49.9	349.18	1647.8	1.9	450.8	349.35	2209.4	3.0
100.4	349.41	1737.3	2.0	500.6	349.12	2267.1	3.0
150.7	349.22	1818.4	2.2	549.2	349.27	2313.8	3.1
200.7	349.68	1892.8	2.4	601.7	349.03	2366.0	3.2
250.9	349.30	1965.0	2.5	651.4	349.59	2412.5	3.3
300.4	349.22	2029.7	2.6	704.5	349.72	2445.1	3.4
349.8	349.32	2091.6	2.7				

with:

$$u(\tau_u) = \frac{8.00 \cdot 10^{-10}\ \mathrm{s}^{-1}}{2\sqrt{3}} = 2.31 \cdot 10^{-10}\ \mathrm{s}^{-1}$$

$$\text{and} \quad u(\tau_{\mathrm{rep}}) = \frac{\sigma_\tau}{\sqrt{3}} \tag{11}$$

The standard deviation between three values obtained for τ_{cal} gave a σ_τ-value of about $8.30 \cdot 10^{-9}$ s at 50 MPa and temperatures $T \geq 273.15$ K and at most $1.67 \cdot 10^{-8}$ s in the rest of cases. The standard deviation σ_τ between three values obtained for τ_p at different pressures did not follow a clear tendency as a function of pressure; thus the maximum standard deviation found was chosen to estimate $u(\tau_{\mathrm{rep}})$ at pressure p, and this σ_τ-value was at most $1.8 \cdot 10^{-8}$ s.

$u(w_{\mathrm{cal}})$ represents the uncertainty in the speed of sound of the IAPWS-95, which at the calibration pressures was less than or equal to 0.1 %. Thus, we considered the maximum uncertainty in $u(w_{\mathrm{cal}})$, that is, 0.1 %.

The uncertainty in temperature measurements $u_c(T)$ could lead to a change in the speed of sound less than dw_{uT} = 0.7 $m \cdot s^{-1}$. The uncertainty in pressure measurements $u_c(p)$ could lead to a change in the speed of sound less than dw_{up} = 3.6 $m \cdot s^{-1}$. This change was dependent on pressure, and its associated uncertainty was calculated with a third-degree polynomial equation. Thus, the respective uncertainty contributions are:

$$u(w_{uT}) = \frac{dw_{uT}}{\sqrt{3}} \tag{12}$$

and

$$u(w_{up}) = 6.90 \cdot 10^{-9} \cdot (p/\mathrm{MPa})^3 - 1.11 \cdot 10^{-5} \cdot (p/\mathrm{MPa})^2 + 7.44 \cdot 10^{-3} \cdot (p/\mathrm{MPa}) \tag{13}$$

To summarize, the uncertainty in the speed of sound, $u_c(w)$, is mainly due to the calibration of the distance between piezoelectric pieces, repeatability of time-of-flight measurements under pressure, and to the calibration of pressure and temperature sensors. $u(w)$ contributes to $u_c(w)$ in about double that of $u(w_{up})$. At pressures from 100 MPa, $u(w_{up})$ becomes higher than $u(w_{uT})$.

Finally, taking into account all of the referred uncertainty components, the combined standard uncertainty in the speed of sound as a function of pressure is:

$$u_c(w) = \left[u^2(w) + u^2(w_{uT}) + u^2(w_{up})\right]^{1/2} \tag{14}$$

This yields a relative standard uncertainty between (0.11 and 0.16) %, which is mainly dependent on pressure. The relative

Table 2. Experimental Speed of Sound in Water at 273.15 K and below

p / MPa	T / K	w / $m \cdot s^{-1}$	$u_c(w)$ / $m \cdot s^{-1}$	p / MPa	T / K	w / $m \cdot s^{-1}$	$u_c(w)$ / $m \cdot s^{-1}$
			T = 253.15 K				
198.9	252.57	1683.1	2.5	225.0	252.55	1736.1	2.6
205.2	252.50	1695.9	2.5	230.0	252.53	1745.4	2.6
210.1	252.52	1705.8	2.6	235.2	252.54	1755.1	2.7
215.3	252.53	1716.3	2.6	239.2	252.54	1762.7	2.7
220.3	252.61	1726.3	2.6	245.0	252.54	1774.1	2.7
225.1	252.59	1735.8	2.6	199.4	252.57	1684.1	2.5
230.0	252.53	1745.0	2.6	204.9	252.56	1695.4	2.5
235.1	252.51	1754.9	2.7	209.9	252.50	1705.2	2.6
240.0	252.50	1764.3	2.7	215.1	252.47	1715.3	2.6
244.9	252.52	1773.9	2.7	220.0	252.47	1725.1	2.6
200.1	252.53	1685.4	2.5	225.1	252.53	1735.1	2.6
204.8	252.53	1695.3	2.5	229.9	252.57	1744.6	2.6
210.1	252.52	1706.0	2.6	235.2	252.57	1754.8	2.7
215.3	252.50	1716.8	2.6	240.1	252.53	1764.5	2.7
220.2	252.51	1726.7	2.6	245.4	252.51	1774.8	2.7
			T = 258.15 K				
176.2	257.70	1657.4	2.4	325.4	257.68	1932.5	3.0
199.9	257.66	1705.5	2.4	349.3	257.69	1972.1	3.1
225.3	257.59	1755.0	2.5	375.3	257.68	2012.5	3.2
250.2	257.64	1801.3	2.5	176.4	257.69	1657.4	2.4
275.2	257.61	1847.7	2.5	199.5	257.61	1703.9	2.5
300.2	257.67	1890.9	2.5	224.1	257.65	1752.6	2.6
325.0	257.70	1928.5	2.5	249.4	257.67	1799.8	2.7
175.1	257.60	1654.5	2.4	274.4	257.62	1845.4	2.8
199.6	257.69	1704.5	2.5	299.9	257.66	1889.6	2.9
224.6	257.70	1754.0	2.6	325.4	257.70	1932.5	3.0
249.5	257.69	1800.5	2.7	350.0	257.69	1972.9	3.1
276.1	257.65	1848.6	2.8	374.6	257.67	2011.2	3.2
299.7	257.67	1889.4	2.9				
			T = 263.15 K				
150.7	262.76	1629.8	2.3	399.9	262.71	2060.0	3.2
200.8	262.81	1728.7	2.5	425.6	262.74	2097.8	3.3
250.6	262.68	1820.4	2.7	450.5	262.74	2133.0	3.4
299.8	262.63	1906.0	2.9	126.3	262.77	1578.6	2.2
350.6	262.76	1986.4	3.1	149.8	262.81	1626.1	2.3
399.7	262.78	2061.2	3.2	174.8	262.77	1676.9	2.4
124.1	262.74	1574.1	2.2	199.8	262.76	1724.8	2.5
148.4	262.76	1623.4	2.3	224.8	262.65	1771.8	2.6
174.8	262.77	1677.2	2.4	249.7	262.73	1816.5	2.7
199.8	262.74	1725.4	2.5	274.5	262.75	1860.6	2.8
224.6	262.76	1772.3	2.6	299.6	262.74	1903.2	2.9
251.0	262.76	1819.5	2.7	324.5	262.71	1944.4	3.0
274.6	262.72	1861.2	2.8	349.4	262.71	1982.7	3.1
299.4	262.73	1903.1	2.9	375.1	262.76	2023.0	3.2
324.6	262.73	1945.1	3.0	399.3	262.76	2058.1	3.2
349.6	262.73	1984.2	3.1	424.3	262.72	2095.3	3.3
374.3	262.72	2023.2	3.2	449.4	262.74	2130.8	3.4

Table 2. Continued

p / MPa	T / K	w / $m \cdot s^{-1}$	$u_c(w)$ / $m \cdot s^{-1}$	p / MPa	T / K	w / $m \cdot s^{-1}$	$u_c(w)$ / $m \cdot s^{-1}$
			T = 268.15 K				
100.5	267.84	1554.9	2.1	349.7	267.87	1997.5	3.1
150.8	267.88	1652.5	2.3	399.7	267.86	2071.2	3.2
199.9	267.89	1745.2	2.5	450.7	267.84	2144.1	3.4
249.6	267.87	1835.0	2.7	500.1	267.84	2209.7	3.5
299.6	267.88	1919.3	2.9	100.8	267.78	1554.9	2.1
349.5	267.88	1996.1	3.1	149.6	267.79	1648.8	2.3
400.0	267.82	2071.6	3.2	199.5	267.77	1744.1	2.5
449.2	267.87	2142.4	3.4	249.4	267.80	1833.6	2.7
98.5	267.81	1551.2	2.1	300.4	267.78	1918.4	2.9
149.6	267.79	1649.8	2.3	349.7	267.78	1997.2	3.1
199.5	267.84	1744.6	2.5	399.6	267.79	2070.9	3.2
251.1	267.87	1837.5	2.8	449.3	267.80	2141.5	3.4
299.4	267.85	1918.6	2.9	500.4	267.79	2208.8	3.5
			T = 273.15 K				
0.1	273.05	1399.3	1.7	299.9	273.11	1929.5	2.8
49.3	273.01	1483.9	1.7	349.4	273.09	2006.9	3.0
99.8	273.18	1577.5	2.1	399.6	273.12	2079.5	3.1
150.2	273.13	1672.1	2.3	450.5	273.10	2150.3	3.3
200.5	273.02	1762.6	2.5	499.9	273.13	2214.6	3.4
250.7	273.10	1849.0	2.7	550.5	273.10	2281.3	3.5
300.0	273.12	1929.7	2.8	602.1	273.10	2345.3	3.7
349.7	273.13	2007.0	3.0	0.1	273.10	1398.7	1.7
401.0	273.12	2081.2	3.1	50.3	273.03	1485.7	1.8
450.2	273.12	2149.8	3.3	100.5	273.10	1579.6	2.1
500.4	273.10	2215.2	3.4	150.4	273.09	1671.6	2.3
550.2	273.11	2281.4	3.5	200.7	273.08	1763.5	2.5
599.5	273.12	2342.0	3.7	250.6	273.11	1848.7	2.7
0.1	273.09	1399.8	1.7	300.6	273.08	1930.8	2.8
49.2	273.07	1484.0	1.7	350.4	273.10	2009.0	3.0
100.0	273.09	1578.3	2.1	399.7	273.08	2080.1	3.1
150.2	273.09	1671.7	2.3	449.3	273.12	2149.5	3.3
200.3	273.11	1762.7	2.5	499.8	273.07	2214.4	3.4
250.3	273.11	1848.4	2.7	550.3	273.12	2276.8	3.5

expanded uncertainty in speed of sound was calculated with a coverage factor of 2. Then it was comprised between (0.22 and 0.32) %. Since it can be assumed that the possible estimated values of w are approximately normally distributed with approximate standard deviation $u_c(w)$, the unknown value of w is believed to lie in the intervals defined ($2u_c$) with a confidence level of about 95 %.

Results and Comparison with Previous Investigations. The speed of sound in pure water was measured at (253.15, 258.15, 263.15, 268.15, 273.15, 278.15, 288.15, 298.15, 308.15, 318.15, 328.15, 338.15, and 348.15) K and at different pressures in the range of stability of liquid water. The results are shown in Table 1 for temperatures above 273.15 K and in Table 2 for 273.15 K and below. As expected, speed of sound increases with increasing pressure and with increasing temperature. Since our data and those from the literature[4,5,10,13,15−18] were not measured at exactly the same pressure and temperature, the IAPWS-95 was taken as a common reference for comparison.

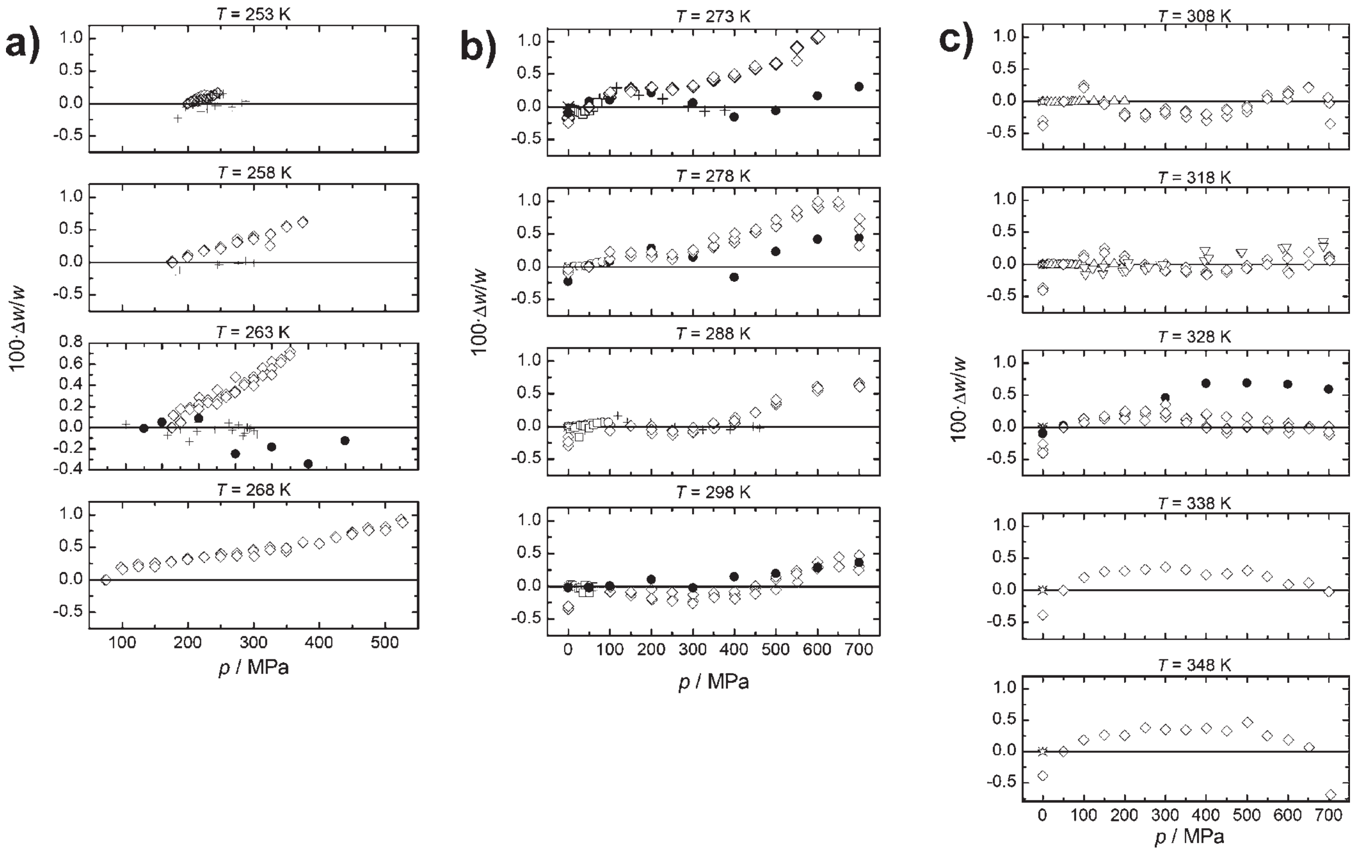

Figure 3. Fractional deviations $\Delta w = w(\text{expt}) - w(\text{calc})$ of the experimental speed of sound $w(\text{expt})$ from values $w(\text{calc})$ calculated using the IAPWS-95 formulation, as a function of pressure at different temperatures. (a) Temperatures below water freezing point at 0.1 MPa. (b) Temperatures from water freezing point to room temperature. (c) Temperatures above room temperature. ◇, this work. Literature data from: +, Petitet et al. (ref 5) at (253, 256, 263, 273, and 292) K; ●, Vance and Brown (ref 13) at (263, 273, 283, 294, and 323) K; ○, Wilson (ref 4) at (283, 292, and 322) K; ×, Del Grosso and Mader (ref 15) at (273, 278, 293, 298, 308, 323, 333, 343, and 348) K; □, Mamedov (ref 16) at (273, 283, 293, and 303) K; ☆, Fujii and Masui (ref 17) at (292, 298, 308, 318, 328, 338, and 348) K; △, Fujii (ref 18) at (313 and 323) K; ▽, Holton (ref 10) at 323 K.

Figure 3 shows the results of the corresponding relative deviations grouped by temperature ranges: below water freezing point at 0.1 MPa (253 to 268) K in Figure 3a, above it and near room temperature (273 to 298) K in Figure 3b, and above room temperature (308 to 348) K in Figure 3c. Data from literature which differ from the temperature of our measurements by 5 K at most have been also included. Compared to data from other authors, the agreement is within experimental uncertainties except at some pressures for (258.15, 263.15, 273.15, and 278.15) K isotherms, or the closest temperatures available for comparison. At low pressures, speeds of sound are systematically underestimated. This confirms that the presence of air in the sample dramatically affects the value of the speed of sound at very low pressure (see the previous comment in the Calibration section). At high pressure, while the calculated values were not extrapolated, the relative deviations between experimental and calculated values were usually below 0.3 %, that is to say, mainly within the tolerance given by IAPWS-95 formulation. The highest relative deviations (1 % at most) appeared around 600 MPa at temperatures below 288.15 K for extrapolated data. The relative deviations used to be positive though there was no systematic tendency with pressure. Nevertheless, it seems that the relative deviation increased roughly linearly with pressure at the lowest temperatures studied. This was also the case for the experimental data from Petitet et al.,[5] at least for (253.15 and 256.15) K. Our analysis confirms that the

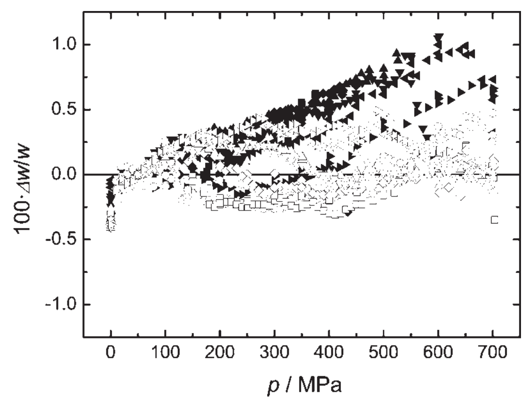

Figure 4. Fractional deviations $\Delta w = w(\text{expt}) - w(\text{calc})$ of the experimental speed of sound $w(\text{expt})$ from values $w(\text{calc})$ calculated using the IAPWS-95 formulation, as a function of pressure at different temperatures. ●, T = 253.15 K; ■, T = 258.15 K; ♦, T = 263.15 K; ▲, T = 268.15 K; ▼, T = 273.15 K; ◀, T = 278.15 K; ▶, T = 288.15 K; ○, T = 298.15 K; □, T = 308.15 K; ◇, T = 318.15 K; △, T = 328.15 K; ▽, T = 338.15 K; ◁, T = 348.15 K; ▷, T = 358.15 K.

predictions of speed of sound from the IAPWS-95 formulation differ from actual values by 1 % in the pressure−temperature regions where few data were available at the time of equation-of-state fitting. In contrast with the results of Vance and Brown[13] we find systematic deviations from the IAPWS-95 formulation at temperatures below room temperature. This trend can be checked in Figure 4 which compiles the deviations for all temperatures as a function of pressure (full symbols).

CONCLUSIONS

The database for speed of sound in water now includes values in the pressure range (0.1 to 700) MPa at temperatures from (253.15 to 348.15) K. The expanded relative uncertainty in speed of sound was estimated to be between (0.22 and 0.32) % depending on pressure with a confidence level of 95 % ($k = 2$). A comparison with available data from other authors shows a global agreement within experimental uncertainties. Analyzing residuals to the IAPWS-95 formulation makes some discrepancies up to 1 % appear in the region where data are extrapolated. The new data set presented in this work offers the possibility to reduce the uncertainty (tolerance) for the speed of sound calculated from the current equation of state for water. This could be made including also specific volume data for water recently determined with the same high pressure equipment and pressure sensor.[19] We hope that our investigations will serve to improve future formulations of the IAPWS-95 equation of state.

AUTHOR INFORMATION

Corresponding Author

*Tel.: +34 91 544 56 07; fax: +34 91 549 36 27. E-mail address: bguignon@ictan.csic.es (B.G.).

Funding Sources

This work has been supported by MICINN through the projects CSD2007-00045 and CTQ2009-14596-C02-01 and by Comunidad de Madrid through the project QUIMAPRES S2009/PPQ-1551. B.G. has a contract from CSIC (JAE Program). E.H. B. acknowledges a FPI grant from Spanish MICINN.

Notes

[§]E-mail: ehidalgob@quim.ucm.es (E.H.B.); mtaravil@quim.ucm.es (M.T.); vgbaonza@quim.ucm.es (V.G.B.); psanz@ictan.csic.es (P.D.S.).

REFERENCES

(1) Marsh, K. N. Role of reference materials for the realization of physicochemical properties. Past, present, and future. *Pure Appl. Chem.* **2000**, *72*, 1809–1818.

(2) Wagner, W.; Pruß, A. The IAPWS Formulation 1995 for the thermodynamic properties of ordinary water substance for general and scientific use. *J. Phys. Chem. Ref. Data* **2002**, *31*, 387–535.

(3) Povey, M. J. W. Ultrasonics in food engineering. Part II: Applications. *J. Food Eng.* **1989**, *9*, 1–20.

(4) Wilson, W. D. Speed of sound in distilled water as a function of temperature and pressure. *J. Acoust. Soc. Am.* **1959**, *31*, 1067–1072.

(5) Petitet, J. P.; Tufeu, R.; Le Neindre, B. Determination of the thermodynamics properties of water from measurements of the speed of sound in the temperature range 251.15−293.15 K and the pressure range 0.1−350 MPa. *Int. J. Thermophys.* **1983**, *4*, 35–50.

(6) Benedetto, G.; Gavioso, R. M.; Giuliano Albo, P. A.; Lago, S.; Madonna Ripa, D.; Spagnolo, R. Speed of sound in pure water at temperatures between 274 and 394 K and at pressures up to 90 MPa. *Int. J. Thermophys.* **2005**, *26*, 1667–1680.

(7) Wiryana, S.; Slutzky, L. J.; Brown, J. M. The equation of state of water to 200 °C and 3.5 GPa: model potentials and the experimental pressure scale. *Earth Planet. Sci. Lett.* **1998**, *163*, 123–130.

(8) Descremps, F.; Datchi, F.; Poilan, A. Hypersonic velocity measurement using Brillouin scattering technique. Application to water under high pressure and temperature. *Ultrasonics* **2006**, e1495–e1498.

(9) Asahara, Y.; Murakami, M.; Ohishi, Y.; Hirao, N.; Hirose, K. Sound velocity measurement in liquid water up to 25 GPa and 900 K: implications for densities of water at lower mantle conditions. *Earth Planet. Sci. Lett.* **2010**, *289*, 479–485.

(10) Holton, G.; Hagelberg, M. P.; Kao, S.; Johnson, W. H., Jr. Ultrasonic-Velocity measurements in water at pressures to 10000 kg/cm^2. *J. Acoust. Soc. Am.* **1968**, *43*, 102–107.

(11) Heydemann, P. L.; Houck, J. C. Self-consistent ultrasonic method for determination of equation of state of liquids at very high pressures. *J. Appl. Phys.* **1969**, *40*, 1609–1613.

(12) Barlow, A. J.; Yazgan, E. Pressure dependence of the velocity of sound in water as a function of temperature. *Brit. J. Appl. Phys.* **1967**, *18*, 645–651.

(13) Vance, S.; Brown, J. M. Sound velocities and thermodynamic properties of water to 700 MPa and −10 to 100 °C. *J. Acoust. Soc. Am.* **2010**, *127*, 174–180.

(14) Guignon, B.; Otero, L.; Molina-García, A. D.; Sanz, P. D. Liquid water−ice I phase diagrams under high pressure: Sodium chloride and sucrose models for food systems. *Biotechnol. Prog.* **2005**, *21*, 439–445.

(15) Del Grosso, V. A.; Mader, C. W. Speed of sound in pure water. *J. Acoust. Soc. Am.* **1972**, *52*, 1442–1146.

(16) Mamedov, A. M. Velocity of ultrasound in water over a wide range of temperatures and pressures. *Inzh. Fiz. Zh.* **1979**, *36*, 156–160.

(17) Fujii, K.; Masui, R. Accurate measurements of the sound velocity in pure water by combining a coherent phase-detection technique and a variable path-length interferometer. *J. Acoust. Soc. Am.* **1993**, *93*, 276–282.

(18) Fujii, K. Accurate measurements of the sound velocity in pure water under high pressure. *12th Symposium on Thermophysical Properties*, Boulder, CO, 1994.

(19) Guignon, B.; Aparicio, C.; Sanz, P. D. Specific volume of water from (253.15 to 323.15) K and pressures up to 350 MPa by volumetric measurements. *J. Chem. Eng. Data* **2010**, *55*, 3338–3345.